

FABRIC EVOLUTION AND GEOCHEMICAL CHARACTERS OF THE MIGMATITES AND ASSOCIATED GNEISSES OF WADI BABA AND WADI DAFARI, WEST CENTRAL SINAI, EGYPT

EL AREF, M.M.; ABD EL WAHID, M. and KABESH, MONA
*Geology Department, Faculty of Science,
Cairo University.*

ملخص

يختص هذا البحث بدراسة صخور الميجماتيت المتواجدة في وادي بعبع ووادي دافري شرق أبو زنيمة بسيناء ، مصر . وقد تم دراسة الأنسجة الصخرية المختلفة لهذه الصخور وتطورها نتيجة عمليات التحرف المختلفة وتواجد درجات مختلفة من الانصهار الجزئي . الدراسة الميجاسكوبية والميكروسكوبية وكذلك التحليل الكيميائي لمكونات الميجماتيت المختلفة وتشمل الباليوسوم الميلانوسوم والليكوسوم أدت إلى الاستدلال على بعض العمليات المصاحبة لتكوين هذه الصخور . وقد تم استنتاج أن صخور الميجماتيت ذات التركيب الستروماتى قد تكونت نتيجة التحول التفاضلى مع تركيز وهجرة لبعض العناصر في نظام شبه مغلق ، أما صخور الميجماتيت ذات التركيب الشريطى والافئالى فقد اقترح تكوينها نتيجة الاحلال الميتاسوماتى فى وجود درجة بسيطة من الانصهار الجزئى والميجماتيت ذات التركيب الشيليرين والحشوى فاستنتج تكوينها تحت تأثير درجة عالية من الانصهار الجزئى .

ABSTRACT

Heterogeneous migmatitic rocks are recorded in Wadi Baba and Wadi Dafari, east of Abu Zenima, Sinai, Egypt. The different migmatitic fabrics and the possible transitional or combined forms, related to brittle or ductile deformation or generated through progressive stages of melting are deduced . Detailed macroscopic and microscopic studies and geochemical characteristics of the fabric components (paleosome, melanosome and leucosome) of the migmatite types throw light on the possible migmatization processes. The stromatic migmatites are suggested to be developed in a locally closed system by metamorphic differentiation and segregation. The

development of the banded ophthalmitic structures, suggests internal metasomatism aided by a limited amount of melt. The migmatites of boudinage and schlieren structures involve a higher degree of partial melting.

INTRODUCTION

The southern part of Sinai peninsula comprises the northern most part of the Precambrian Arabo-Nubian crystalline massif. The northwestern extremity of the exposed basement rocks in West Central Sinai (Fig. 1) is occupied mainly by metamorphic rocks, diorites and old granitoids. They are intruded by younger pink granites and dykes of different compositions and trends. The basement rocks were uplifted, peneplained and overlain by Cambro-Ordovician and Carboniferous sediments.

Rocks with heterogeneous character, showing migmatitic fabrics are recorded in Wadi Baba and Wadi Dafari at the western part of the basement exposures (Fig. 1). The main structural types of the observed migmatites are: stromatic, banded, boudinage, ophthalmitic (augen) and schlieren. These structural types are described and discussed in detail, with emphasis on the evolution of the different fabrics and the possible transitional or combined forms, related to brittle or ductile deformation or generated through progressive stages of melting. The possible mechanisms involved during the migmatization processes are discussed through the recognition of the macroscopic, microscopic and geochemical characters of the main fabric units of the different migmatite types. The main fabric units are distinguished according to the description of Mehnert (1968); Yardley (1978); Johannes and Gupta (1982 and 1983). In the present study the term stromatic is used to describe irregular, discontinuous lamellae segregated parallel to the main foliation of the gneiss. Whereas, banded refer to more straight continuous alternating bands.

MIGMATITES OF WADI BABA

At the southern part of Wadi Baba, Wadi Abu Hamata and Wadi Samra, the exposed gneisses exhibit signs of migmatization. The migmatized gneisses are recorded as large masses enclosed in the old granitoids and intruded by pink granites (Fig. 1). The migmatization effect is represented by the formation of segregations of light leucosomes in the form of thin lamellae parallel to the main foliation *S* of the host rocks, giving them a well developed stromatic structure. The migmatitic banding is harmonically folded, showing tight and isoclinal folds (Pl. 1, Fig. a). Microscopically, the mesosomes are medium grained biotite gneiss or cordierite - biotite gneiss (Pl. I, Fig. b). The leucosome lamellae consist of coarse grained quartz and plagioclase crystals showing hypidiomorphic granular texture (Pl. I, Fig. b). Very thin discontinuous lamellae of cordierite - biotite gneiss (Pl. I, Fig. b).

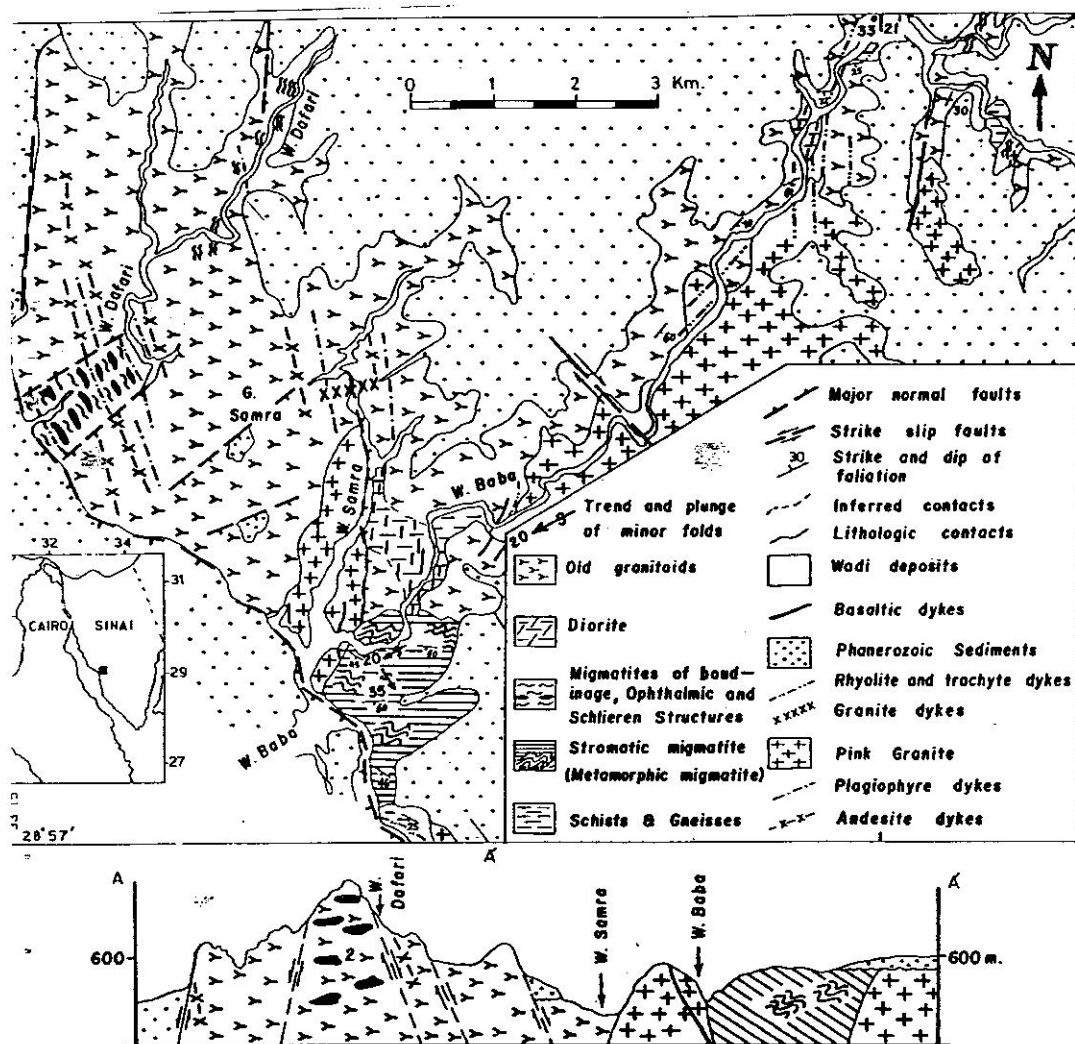


Fig.(1) GEOLOGICAL MAP OF THE AREA EAST OF ABU ZENIMA SHOWING THE LOCATION OF THE STUDIED MIGMATITE EXPOSURES.

MIGMATITES OF WADI DAFARI

At the western part of Wadi Dafari migmatitic rocks form large lenticular masses and elongated bands of black, brown, purple and light pink colours. The dark bodies are amphibolites, hornblende-biotite schists and fine grained banded gneisses enclosed in the granodiorites and occasionally surrounded by light migmatitic material. The outcrop of the migmatitic rocks is structurally controlled, being bounded to the west by a major NNW fault zone, and is delimited to the north and south by ENE trending faults (Fig. 1). These migmatites are grouped into the following structural types :

(a) migmatites of banded structure

(b) migmatites of banding and dilatation structure

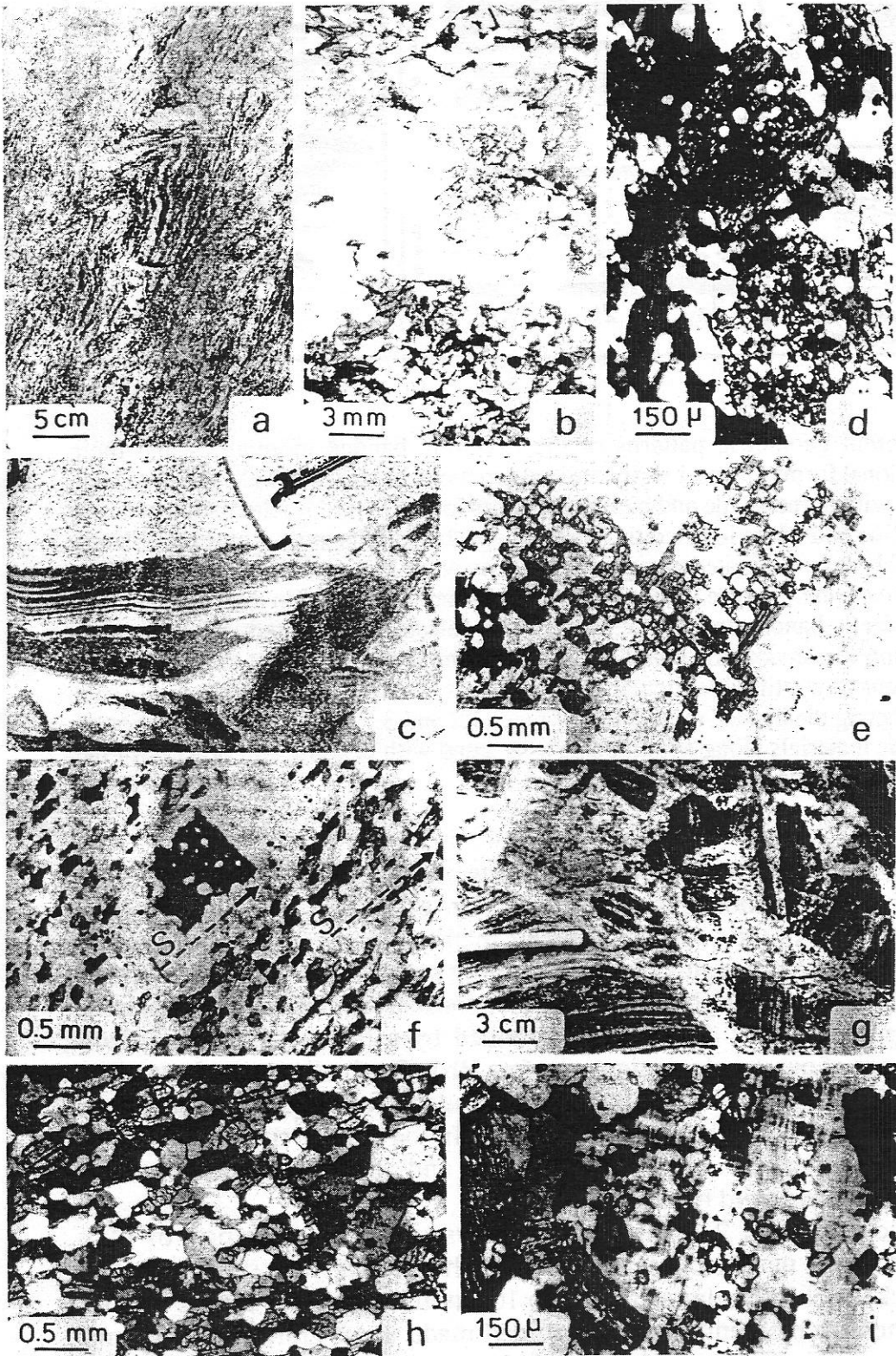
Banded Gneisses and Migmatites of Banded Structure

The studied banded rocks consist of rhythmically alternating dark and light bands and lamellae (Pl. 1, Fig. c). They vary in thickness from 1 mm to few cms, generally regular, with well defined contacts and uniform thickness or may pinch out laterally forming small lenticles, or affected by faulting (Fig. 2). These banded rocks have sharp contacts with the host granodiorite that surround and intrude them (Pl. I, Fig. c) and represent fine grained banded gneiss (Fig. 2, type 1) and rocks showing signs of migmatization (Fig. 2, types 2-5).

Microscopically, type 1 in Figure 2 consists of rhythmic bands and lamellae which can be expressed as "12131" and "1212" rhythmical systems (Figs. 3A and 3B, respectively). The repeated bands and lamellae are made up of different proportions, grain sizes and forms of hornblende, biotite, quartz, plagioclase and occasional sillimanite. Combinations of these two rhythmic types are common. In the former rhythmic type, the dark fine band (band No. 1 in figure 3A) is formed of fine oriented hornblende and biotite (Hb1 and Bi1), up to 0.2 mm in size, constituting the main foliation S, with subordinate quartz and plagioclase. The second bands (band No. 2 in figure 3A) are lighter in colour and consist of large hornblende porphyroblasts (Hb2), up to 2 mm in diameter, and fine biotite (Bi1) in a fine to medium grained quartzofeldspathic matrix with fine hornblende (Hb2). These bands exhibit some variations in the grain size and frequency of some minerals. They show increase in the grain size of the matrix with decrease in the frequency of Bi1 and Hb1 accompanied by increase in the grain size of Hb2 porphyroblasts, from 0.5 mm up to 2 mm in diameter (Pl. I, Figs. d and e) and decrease in their degree of idiomorphism. The Hb2 enclose rounded quartz and opaques that show increase in grain size and frequency with the increase of the grain sizes of the porphyroblasts. The rounded

Plate 1

- a : Stromatic migmatite of W. Baba, showing isoclinal tight folds.
- b : Photomicrograph of the stromatic migmatite, consisting of mesosome as medium grained biotite gneiss and leucosome of coarse grained quartz and plagioclase.
- c : Migmatite of banded structure, showing sharp contact with the granodiorite.
- d : Hornblende porphyroblasts (Hb2) growing in the dark bands of the banded migmatites.
- e : A large hornblende porphyroblast with inclusions of the same size as the surrounding matrix.
- f : Biotite metablast (Bi2) developed in the light band, near the contact with the foliated dark band. The biotite porphyroblast is surrounded by a clear zone.
- g : Close up view of banded migmatite breccia cemented by new generation of light neosome.
- h : Photomicrograph of the hornblende schist bands.



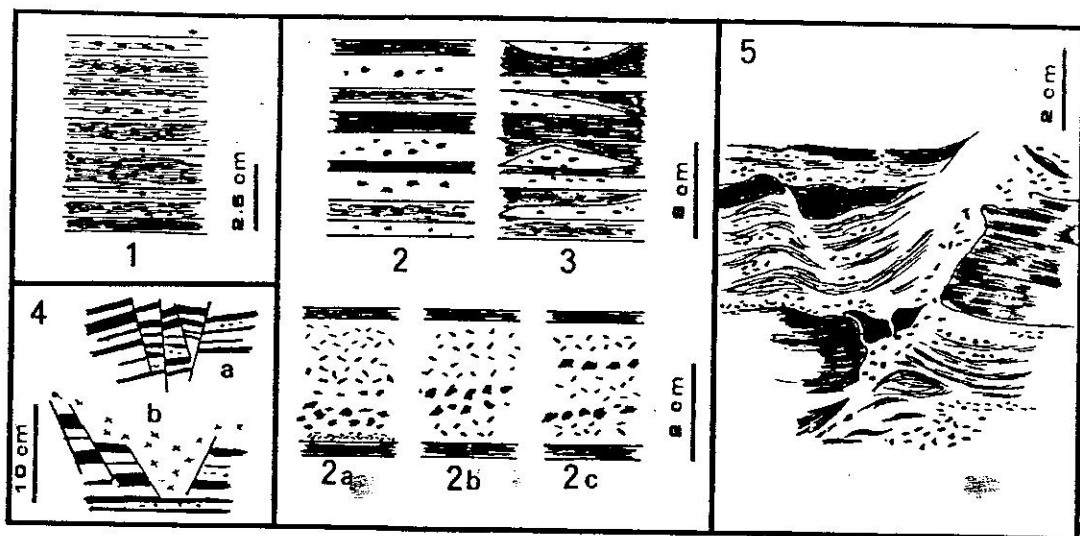


Fig.2

The different geometric patterns of the rhythmic banded migmatites and their deformational forms : Type 1 = rhythmic alternations of dark and light grey bands or lamellae, with hornblende and biotite porphyroblasts ; Type 2 = Alternation of black amphibolitic and white leucocratic bands ; Type 2a exhibits megascopic hornblende porphyroblasts concentrated along the contact between leucosome and the underlying amphibolitic band. In type 2b, the porphyroblasts are distributed in the middle part of the leucocratic bands. In type 2c, the porphyroblasts are arranged in two parallel lines within the leucocratic bands. Type 3 is similar to type 2, but the leucocratic bands occur as stratified lenticular forms. Types 4 a and 4b represent small scale faults affecting the banded migmatites of types 1,2 and 3. Type 5, shows injection of leucocratic materials along a fault plane associated with bending and flowage of the light and dark bands .

inclusions in the large Hb2 porphyroblasts are mainly of the same size as those of the surrounding matrix (Pl. I, Fig. e), suggesting simultaneous recrystallization of the quartzofeldspathic matrix with the progressive growth of Hb2 along grain margins of the surrounding crystals. The third band (band No. 3 in figure 3A) is lighter in colour and consists of biotite porphyroblasts (Bi2), up to 1 mm in diameter, surrounded by a fine partly polygonized groundmass of quartz, plagioclase and few Hb1. The biotite metablasts grow mostly following the main foliation, or at random, forming a clear zone free of fine hornblende and biotite (Pl. I, Fig. f). In the "1212" rhythmic system, the alternating bands are mineralogically and texturally similar to the described first and third bands.

Rocks of type 2 in figure 2 displays rhythmic alteration of black amphibolitic and white leucocratic bands, either regular and straight, up to 3 cm thick, or of lenticular forms, up to 10 cm in length (Fig. 2, type 3). The leucosomes are medium to coarse grained made up of granular quartz and plagioclase and include hornblende and biotite porphyroblasts, up to 5 mm in

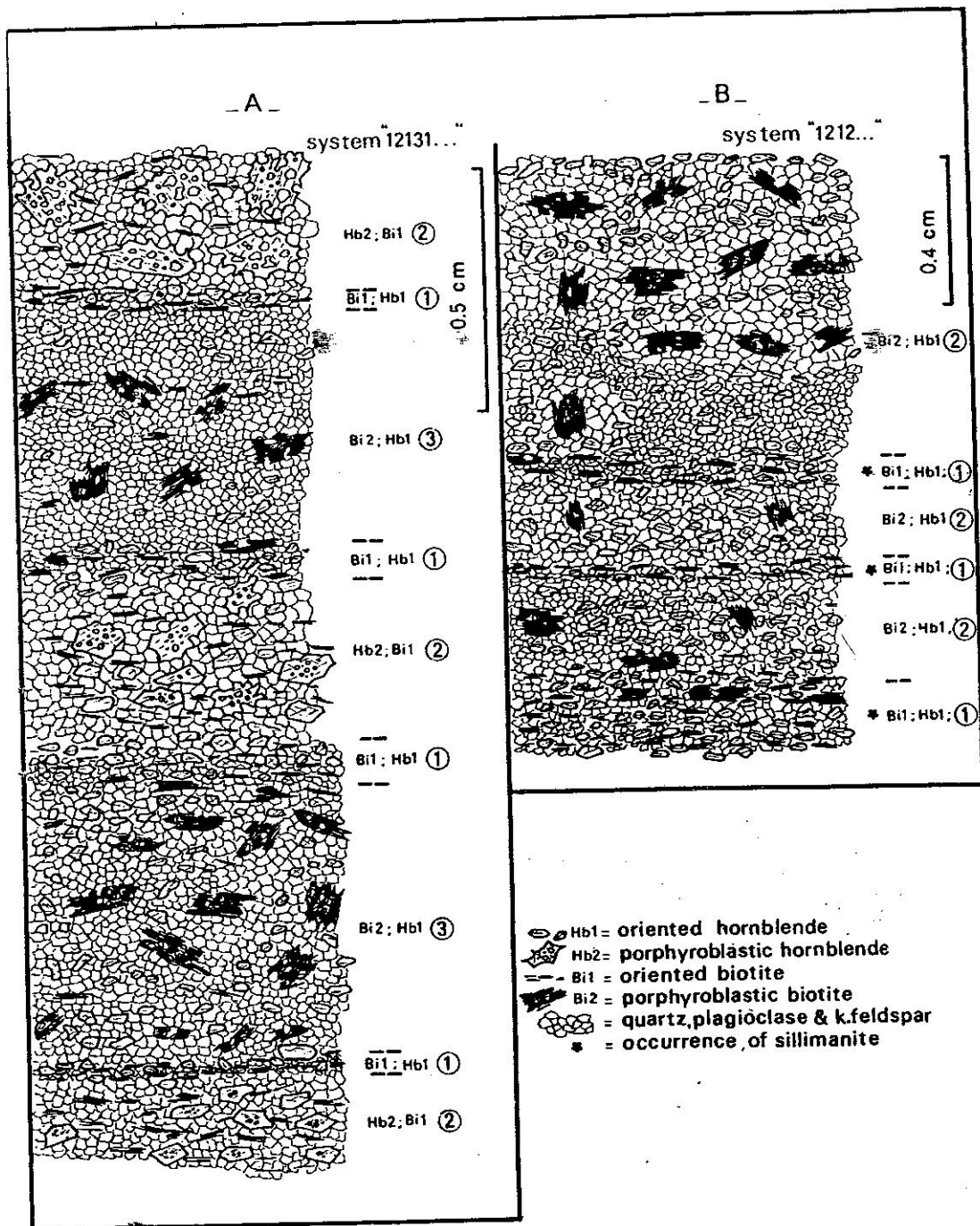


Fig. 3 : Representative microscopic profiles of type 1 in Figure 2. the hornblende and biotite occur in two generations, fine grained subidiomorphic oriented crystals (Hb1 and Bi1) and large

These banded rocks show some deformational features developed during or after the formation of the leucosome. Two types of deformation have been recognized, brittle and melt enhanced deformation. The brittle deformation is represented by the development of sets of vertical and inclined normal faults (Fig. 2, types 4 a and b). The second type of deformation is indicated by the development of leucocratic neosome material along fault planes traversing the migmatite banding. Displacement and bending of the migmatite bands along the fault planes and the formation of a flexure zone, indicate flowage of the leucocratic material during faulting and the development of the neosomes (Fig. 2, type 5). Formation of banded migmatite breccia cemented by neosome (Pl. I, Fig. g), similar in composition and texture to the light bands, indicates progressive stage of partial melting of the leucosome shortly after brittle deformation.

Migmatites of boudinage and dilatation structure

A common fabric is found as boudinaged bands and lenses, representing relicts slightly affected by ultrametamorphism and surrounded by lighter grey migmatitic gneisses or granitoids. The development of this structure depends on the difference in competency of the fabric units, which consist of competent dark bodies surrounded by a less competent and more mobile quartzofeldspathic material. Thus with great difference in the mechanical behaviour of the two parts, the dark bands are commonly broken into boudins that may be ruptured into fragments, tilted and displaced by dilatation and surrounded by mobilized migmatitic leucosomes (Fig. 4). In an advanced stage of ductile deformation, the rafts flatten into smaller lenticular bodies with tapered ends, lying along the foliation of the surrounding migmatitic gneissose leucosome which form flow structure around their edges. Ultimately, the deformation of the dark bodies by rupturing, flattening, dilatation and corrosion, give rise to dark lenses of different sizes, that may become elongated or even highly stretched into thin bands and streaks or grade into a schlieren type with small spindle-shaped inclusions flowing in foliated matrix.

Microscopically, the dark bands and boudins are made mainly of hornblende, biotite-hornblende and biotite schists, showing fine grained granoblastic schistose texture (Pl. I, Fig. h). The dark boudins exhibit large K-feldspar porphyroblasts as stumpy and equant crystals of microcline and perthite, enclosing random fine rounded inclusions of hornblende, quartz and biotite (Pl. I, Fig. i). The dark bands also show signs of modifications, represented by blastic growth of plagioclase (Pl. II, Fig. a) and hornblende enclosing oriented biotite flakes (Pl. II, Fig. b). An advanced stage of modification results in the formation of orthoclase and microperthite blasts exhibiting intergranular growth or occur as subhedral poikiloblasts (Pl. II, Fig. c). The associated leucosome is composed mainly of quartz, plagioclase, orthoclase and perthite, displaying medium grained equigranular texture (Pl. II, Fig. d). Apatite and sphene are the main accessories. Sphene is found as

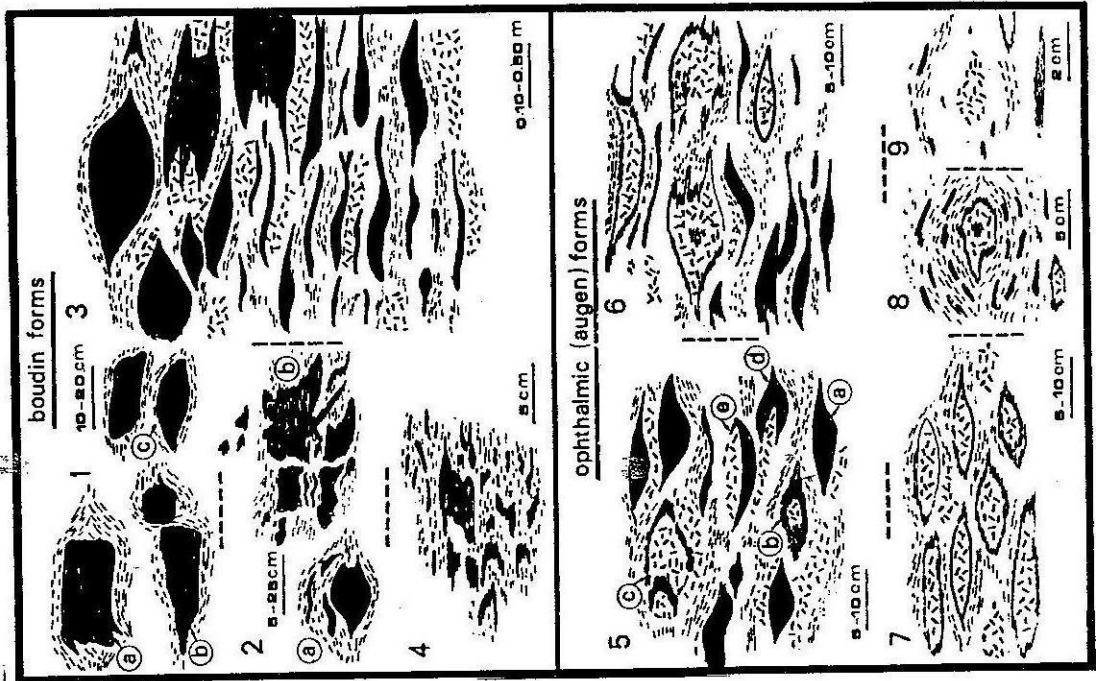


Fig. 4 : Schematic representation showing the evolutionary trend of the boudin and ophthalmic forms : 1a = The initial stage of boudin formation represented by separate dark amphibolitic bodies with angular outlines ; 1b = Boudin ruptured by joints and fractures into fragments tilted and displaced by dilatation, with fine migmatitic leucosomes flowing around them ; 1c = rafts start to flatten with tapered tips ; 2a = lenticular bodies dragging finer dark streaks around them in a foliated fine leucosome ; 2b = large bodies ruptured into irregular fragments, with dilatation and dragging of smaller pieces and streaks ; 3 = progressive deformation of the dark bodies leading to the formation of small lenses, streaks or irregular masses, surrounded by fine foliated and coarse leucosomes ; 4 = amphibolitic boudins, highly eroded, leaving relict streaks and irregular bodies ; 5a = well preserved dark lenses with sharp contacts ; 5b = formation of new coarse grained granitic phase at the core of the lens ; 5c = progressive growth of the leucosome at the core, corroding and replacing the dark material ; 5d and 5e = coarse granitic leucosome surrounded the lenses and streaks or invade them ; 6 = advanced stages of replacement and erosion, showing leucosomes leaving only fine dark streaks at the borders of the replaced lenses, which may include some dark relicts ; 7 = replaced lenses formed of coarse granitic material lined by dark borders and surrounded by gneissose leucosome ; 8 = a replaced lens wrapped by foliated migmatitic matrix with dark schlierens ; 9 = coarse anitic lens without a dark envelope wrapped by the light and coarser leucosome leucosome.

Migmatites of ophthalmitic (augen) structure

In some high grade heterogeneous rocks, dark relicts are found as lenses and stretched streaks, surrounded by gneissose granitic leucosomes together with small augens of neosomatic material delimited by mafic streaks as eyelids. The evolutionary trend of the development of these neosomatic material at the expense of the dark paleosomes is shown in figure 4. In the dark lenses a new coarse grained granitic phase starts to generate at the cores and increase progressively replacing the lenses and leaving fine dark streaks at the borders (Pl, II, Fig, e). Thus the formation of ophthalmites may represent modification of the mesosomes and the leucosomes in an advanced stage of migmatization. The mesosomes are represented by medium grained biotite-hornblende or biotite schists modified by the growth of large plagioclase porphyroblasts. The feldspar porphyroblasts grow individually or as crystal aggregates, that cause destruction of the foliation. Under the effect of ultrametamorphism and partial melting, K-feldspar porphyroblasts develop in the biotite schist mesosome. This is accompanied by the decomposition of biotite flakes into iron oxides during dehydration - melting reactions (Busch et al., 1974 ; Ashworth, 1979), where the released K aids in the formation of K-feldspars. In an advanced stage, the leucocratic augens are formed of an aggregate of coarse quartz, plagioclase and biotite. The surrounding fine leucosomes affected by partial melting show growth of separate or aggregated plagioclase and K-feldspar porphyroblasts or elongated lenticles of coarse granite texture.

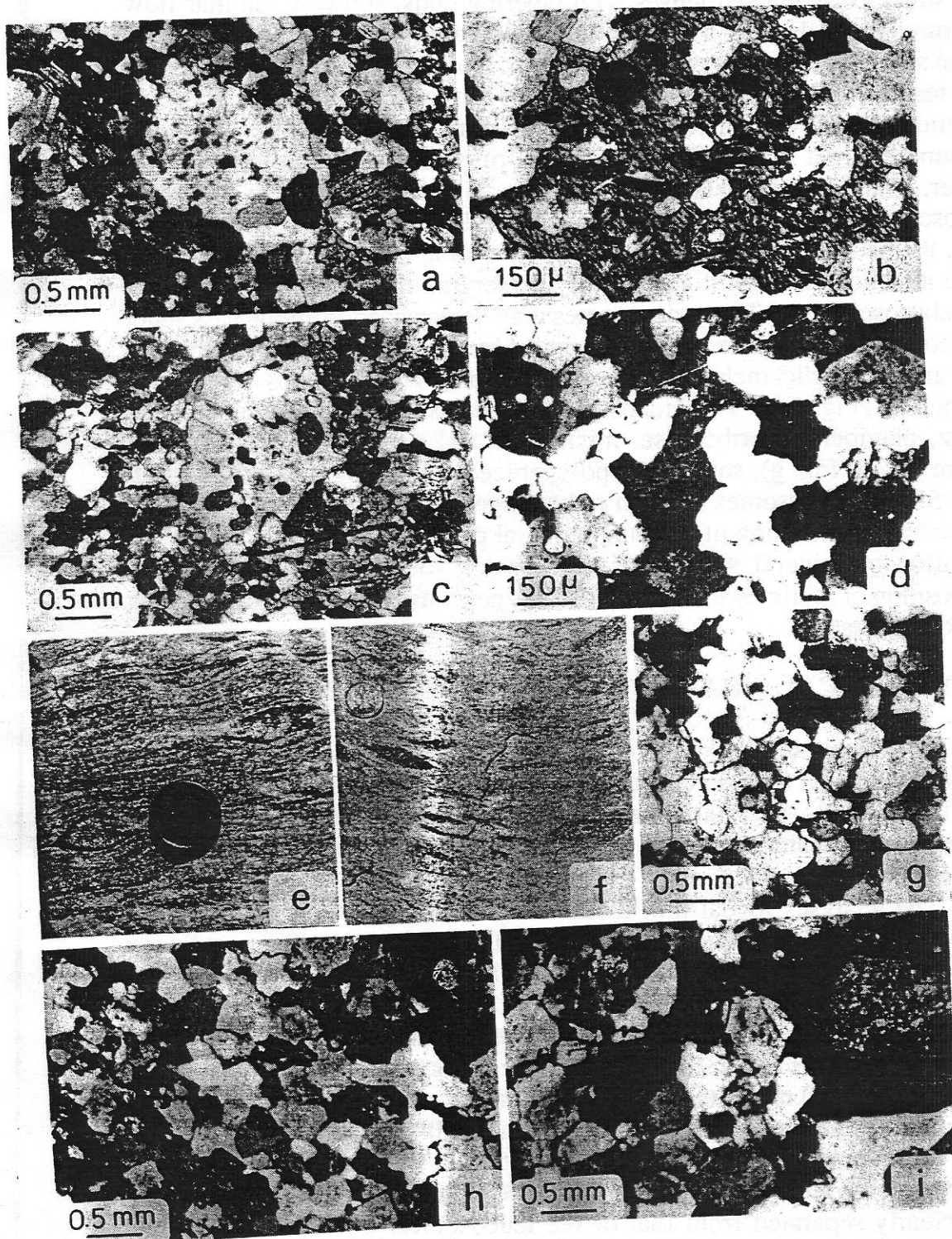
Migmatites of schlieren structure

Rocks with schlieren structure represent the main migmatitic fabric observed in Wadi Dafari, commonly forming the matrix surrounding other structural types, especially the amphibolitic bands and boudins and ophthalmitic structures. These rocks form large exposures surrounded and intruded by gneissose granodiorites. The rocks of this type are of

Plate II

- a : Photomicrograph of the hornblende schist band, showing plagioclase Poikiloblast enclosing fine rounded hornblende and quartz crystals.
- b : Hornblende poikiloblast enclosing rounded quartz and plagioclase and oriented biotite flakes.
- c : Subhedral orthoclase poikiloblast enclosing rounded quartz and hornblende.
- d : Photomicrograph of the granitic leucosome of the boudinage migmatite. The K-feldspar encloses rounded quartz grains.
- e : Close up view of ophthalmic structure, consisting of lenses with coarse leucocratic cores and lined by dark rims.
- f : Migmatite of schlieren structure, showing dark streaks and stretched lenses with laminar flow structure.

Figs. g, h and i : Photomicrographs of the leucosome of the schlieren migmatite, showing rounded and xenomorphic quartz and biotite.



heterogeneous characters and consist of roughly parallel irregular light and dark streaks or stretched lenses with tapering ends, showing laminar flow structure (Pl. II, Fig. f). The dark inclusions are mainly amphibolites and biotite schist (paleosomes or melanosomes), representing resistant relicts that have responded differentially to the processes of migmatization. They become flattened, tapered or twisted, sometimes corroded or digested by the surrounding light migmatitic leucosomes, or modified by the formation of lighter, granitic materials at their cores. The heterogeneity is reflected microscopically, regarding the composition and texture of the different fabric units, the paleosome, melanosome and leucosome (Fig. 5). Paleosomes are found as relict lenses (restites), mostly preserving the original composition and schistose texture. The melanosomes may be detached from the dark relict paleosome and is mechanically incorporated by the advance of the leucosome. They are either relict melanosomes or formed of new generations of biotite or hornblende (Fig. 5A). The leucosomes consist of fine to medium grained quartz, plagioclase, orthoclase, microcline and perthite, of granoblastic texture (Pl. II, Fig. g), sometimes polygonized (Pl. II, Fig. h). As shown in Fig. 5B, the leucosomes are also of heterogeneous character, displayed by the variable distribution of the main mineral phases. This is reflected by the formation of mineral aggregates, or through local modification of the composition or fabric by the growth of later generations of the main minerals and polygonization.

GEOCHEMICAL CHARACTERISTICS OF THE MIGMATITES

The analysed samples of the migmatites are chosen so as to represent the paleosome and leucosome of the different structural types (Table 1). The analytical results are statistically processed by linear regression and computerized cluster analyses, and portrayed by variation diagrams and dendrograms.

The analyses reveal that the heterogeneous character of the fabric components is mainly expressed by variation in some major oxides as SiO_2 , Fe_2O_3 and MgO , some trace elements as Zr and Ba and rare earths as La and Nd. Other oxides as Al_2O_3 , K_2O , Na_2O and CaO do not show great variations between the paleosomes and associated leucosomes of each structural type. This may reflect variations in the original materials and in the degree of chemical mobility of elements in metamorphic condition or during melting. SiO_2 shows a strong negative relation with Fe_2O_3 , MgO , CaO and MnO , and a moderate negative relation with Al_2O_3 and Na_2O , and very weak relation with K_2O (Fig. 6). It is noticed that the paleosomes plot in a field clearly separated from that of the leucosomes. The leucosome field shows high SiO_2 content, with low Fe_2O_3 , MgO , MnO , Al_2O_3 and CaO compared to the paleosome field. On the $\text{Na}_2\text{O} - \text{SiO}_2$ and $\text{K}_2\text{O} - \text{SiO}_2$ diagrams, the Na_2O and K_2O contents of the leucosome and paleosome fields are nearly similar. The biotite schist shows a general intermediate

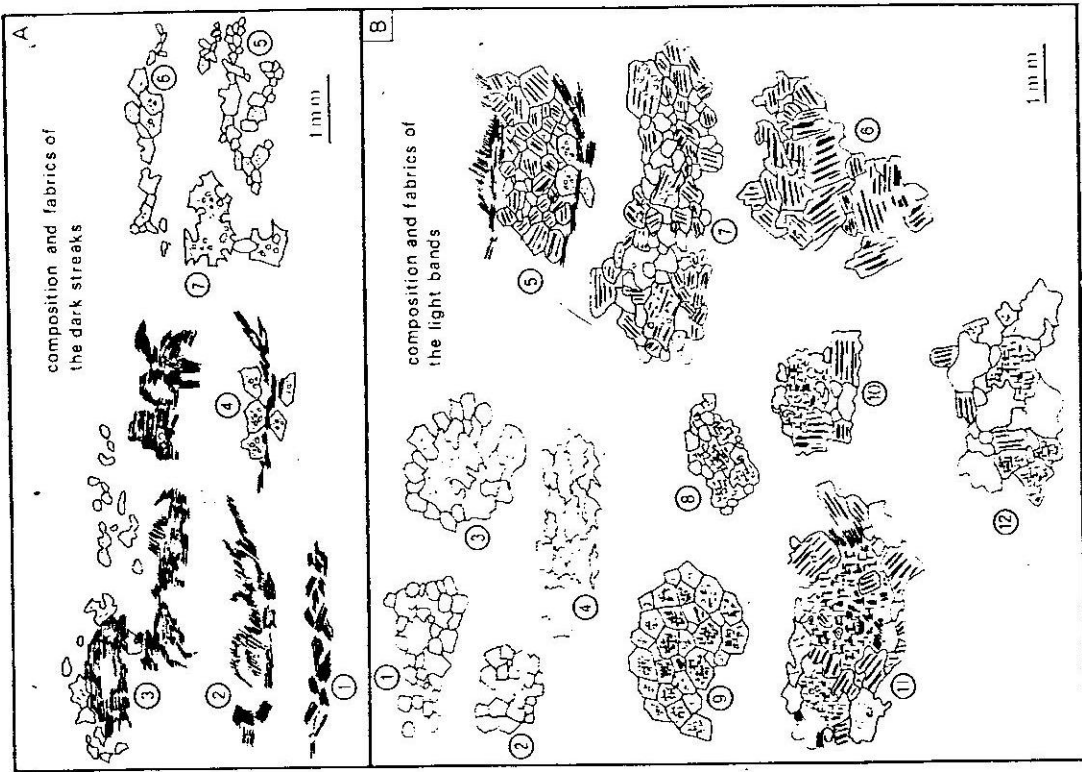


Fig. 5 : The fabric characteristics and composition of the dark and light streaks of the schlieren structure. A1 = preferred oriented fine biotite flakes; A2 = later biotite blasts enclosing some quartz crystals, growing on the contacts of older biotite flakes; A3 = large oriented biotite porphyroblasts; A4 = subhedral hornblende crystals growing all around the oriented biotite flakes; A5 = aligned fine subhedral hornblende crystals; A6 = fine subhedral and large hornblende porphyroblasts; A7 = aggregate of large hornblende porphyroblasts; B1 = crystal aggregate of rounded quartz grains; B2 = quartz crystals showing straight polygonal faces; B3 = aggregate quartz porphyroblasts; B4 = stretched quartz crystals with sutured boundaries; B5 = plagioclase crystals with polygonal outlines; B6 = anhedral to subhedral interlocked plagioclase crystals; B7 = crystal aggregate of euhedral to subhedral plagioclase free of inclusions, plagioclase porphyroblasts and K-feldspars (orthoclase, microcline, perthite) with granular quartz; B8 = K- Feldspar crystal aggregate with granular quartz; B9 = K-feldspar crystal aggregate with polygonized straight crystal faces and triple junctions; B10 = blastitic K-feldspars with plagioclase and quartz; B11 = large poikiloblasts, of K-feldspars with subhedral plagioclase; B12 = typical medium to coarse grained hypidiomorphic granitic texture.

FABRIC EVOLUTION

Table (I) : CHEMICAL ANALYSES OF THE MIGMATITES

Sample No.	Bd ₁	B ₁	B ₂	D 106a	D 132	D 110	D 100	D 106b	D 107	D 108	D
Geometrical type	Biotite gneiss	Stromatic		Banded migmatites							1
	P.	P.	L.	P.	P.	P.	P.	L.	L.	L.	P.
SiO ₂	64.91	61.11	70.71	54.13	59.88	62.98	65.22	70.13	71.14	74.22	60
Al ₂ O ₃	14.03	15.34	14.13	17.54	16.98	15.47	14.75	13.58	14.21	13.05	17
Fe ₂ O ₃	3.20	4.22	1.10	2.18	1.40	1.72	2.08	1.20	1.03	0.06	4
FeO	1.19	1.9	0.80	5.75	4.30	4.19	3.11	0.70	1.98	2.17	0
MnO	0.12	0.14	0.05	0.19	0.09	0.14	0.13	0.05	0.07	0.06	0
MgO	3.21	2.71	0.81	4.06	8.71	2.57	2.7	1.66	1.04	0.78	3
CaO	2.08	2.45	1.08	6.09	8.82	5.21	3.48	1.12	3.75	3.26	3
Na ₂ O	5.07	5.32	5.39	4.68	5.01	4.58	4.46	5.13	4.92	4.58	5
K ₂ O	4.53	4.95	4.61	1.84	1.83	0.91	1.63	4.57	0.62	0.52	1
TiO ₂	0.45	0.47	0.33	0.87	0.99	0.73	0.57	0.46	0.38	0.32	1
P ₂ O ₅	0.10	0.05	0.00	0.25	0.31	0.21	0.18	0.19	0.13	0.12	0
Total	98.89	98.66	99.01	98.86	98.97	99.37	99.4	98.79	99.60	99.45	95
Rb	276	329.3	288	56	62	23	68	208.4	9.10	4.5	35
Sr	514.4	669.9	469	328	525	324	291	489.3	314	361	52
Y	99.7	19.20	19.20	38	22	29	28	119.6	16	22	22
Zr	565.7	621.20	416.4	187	192	177	159	488	127	190	18
Ba	5563	2465	4289	620	739	239	689	5480	181	238	46
La	62.20	15.70	0.00	19	19	24	23	55.80	26	27	26
Nd	16.30	0.00	0.00	31	27	23	24	16.40	17	29	27
Pb	84.60	82	40.9	12	15	14	23	86.10	17	16	17
Th	34	13.40	0.60	1	5	6	11	45.30	9	8	9

P. = Paleosome

L. = Leucosome

NORMATIVE Qz., Or., Ab. OF THE LEUCOSOMES

Sample No.	D 106b	D 107	D 108	D 134c	D 134d	D 104	D 105	D 138	1
Qz.	21.5	40.7	36.6	28.2	31.8	25.9	31.6	31.6	
Or.	30	4.7	3.1	43.3	26.2	28.8	28.4	31	
Ab.	48.3	54.8	38.7	43.3	41.9	45.2	40	37.3	

D 121	D 122	D 134a	D 134b	D 134c	D 134d	D 104	D 105	D 138	D 139	D 131
bands		Boundinage					Schlieren			
P.	P.	P.	P.	L.	L.	L.	L.	L.	L.	L.
59.41	56.08	54.28	55.77	71.49	73.06	72.52	71.63	71.82	70.82	70.31
17.11	14.51	13.68	15.15	13.59	13.86	14.18	13.54	14.46	14.77	14.51
1.09	6.55	7.28	1.39	0.00	0.15	0.22	1.14	0.82	0.64	0.63
4.07	2.51	3.07	6.97	1.81	0.84	1.44	0.81	1.65	1.91	2.11
0.14	0.11	0.21	0.24	0.06	0.03	0.04	0.04	0.05	0.05	0.07
3.73	3.68	4.85	4.03	0.84	0.23	0.53	0.66	0.74	0.42	0.83
3.7	4.86	4.9	5.6	1.42	0.77	1.63	1.65	1.45	1.33	1.93
4.48	5.57	5.74	4.96	2.97	5.03	4.32	4.13	3.84	4.9	4.63
1.99	4.14	4.42	2.59	6.41	4.59	3.86	4.19	4.55	3.46	3.17
0.68	0.32	0.25	0.70	0.25	0.29	0.23	0.43	0.35	0.29	0.36
0.21	0.58	0.56	0.28	0.08	0.00	0.09	0.03	0.12	0.09	0.12
98.24	98.91	99.29	98.98	99.45	98.85	99.5	98.25	100.3	99.32	99.39
70	285	314	48	106	284	66	266	116	81	80
425	865	549.70	249	207	459	261	484.50	247	218	252
18	19.20	44.40	27	33	19.2	17	49	21	26	29
207	269	176.80	43	61	405	234	233	224	286	233
1090	418	440.50	948	1940	3275	1020	3432	1190	924	240
26	279	159	19	6	41.60	35	55.40	31	34	27
27	236	103	16	17	0.00	30	0.00	29	37	31
18	72.80	72	23	23	32.3	27	58.70	27	22	23
7	33.70	27.80	6	3	0.50	11	14	13	9	10

9 D 131

5 30

7 22.7

8 47.3

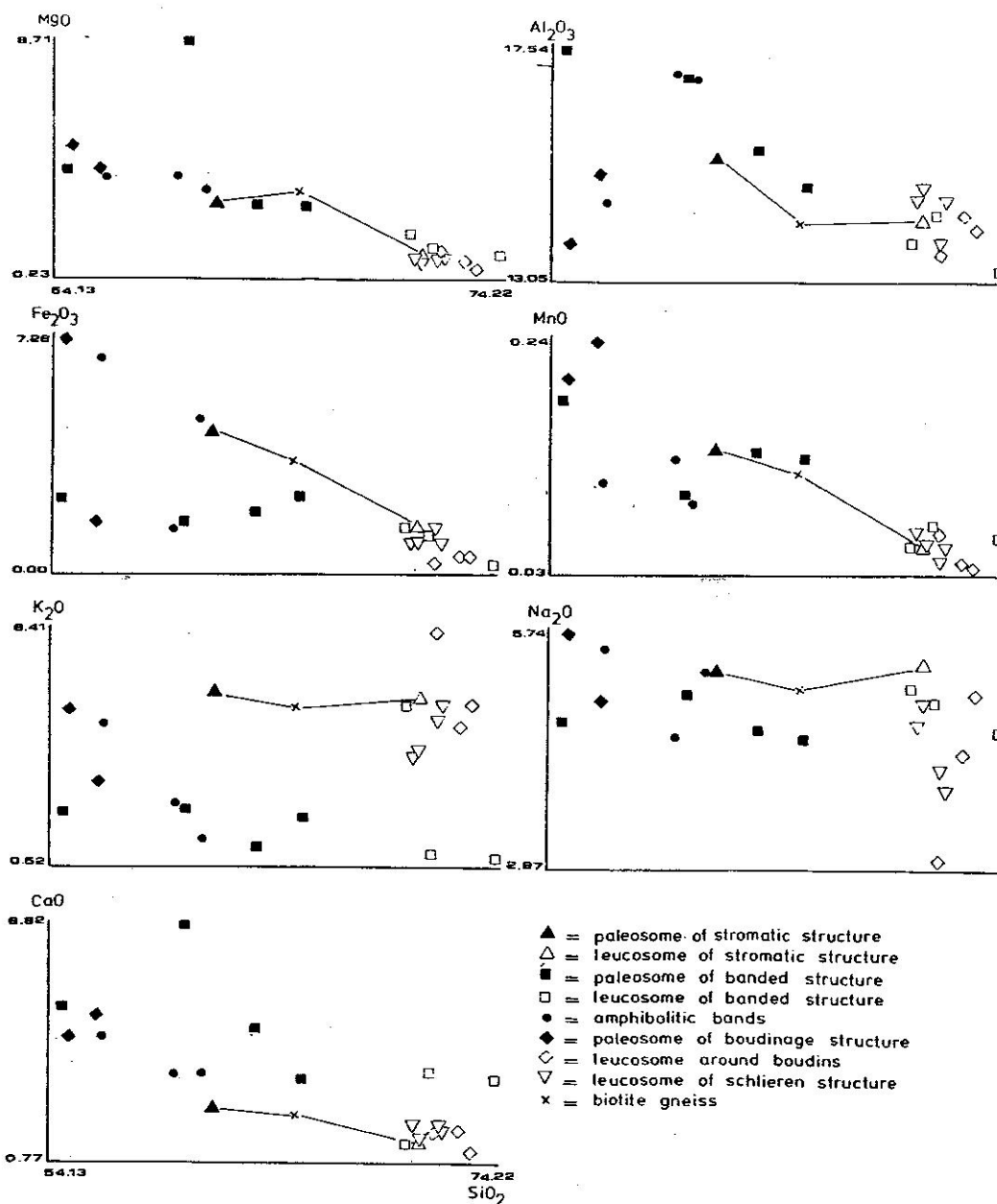


Fig. 6 : Variation diagram of SiO_2 versus major oxides for the studied migmatites and biotite gneiss. The solid line ties the parent biotite gneiss to the corresponding paleosomes and leucosome of the stromatic migmatite.

In figure 7a, the leucosomes mainly plot in a field of high SiO_2 and low $\text{MgO} + \text{FeO}$ and $\text{K}_2\text{O} + \text{Na}_2\text{O}$, whereas the paleosomes show high ferric group. It is clearly observed that there is no great variation in the $\text{K}_2\text{O} + \text{Na}_2\text{O}$ content of the leucosomes and paleosomes, suggesting a closed system concerning these elements together relative to the SiO_2 and Ferric Group. The leucosomes of banded structure show rather high ferric content and plot away from the leucosome field, which can be attributed to the occasional growth of hornblende and biotite porphyroblasts. In Figure 7b, the amphibolitic paleosomes show high values of CaO than the leucosomes, which on the other hand have higher K_2O content. It is also clear that Na_2O values are similar in the paleosomes and leucosomes. The lower values of

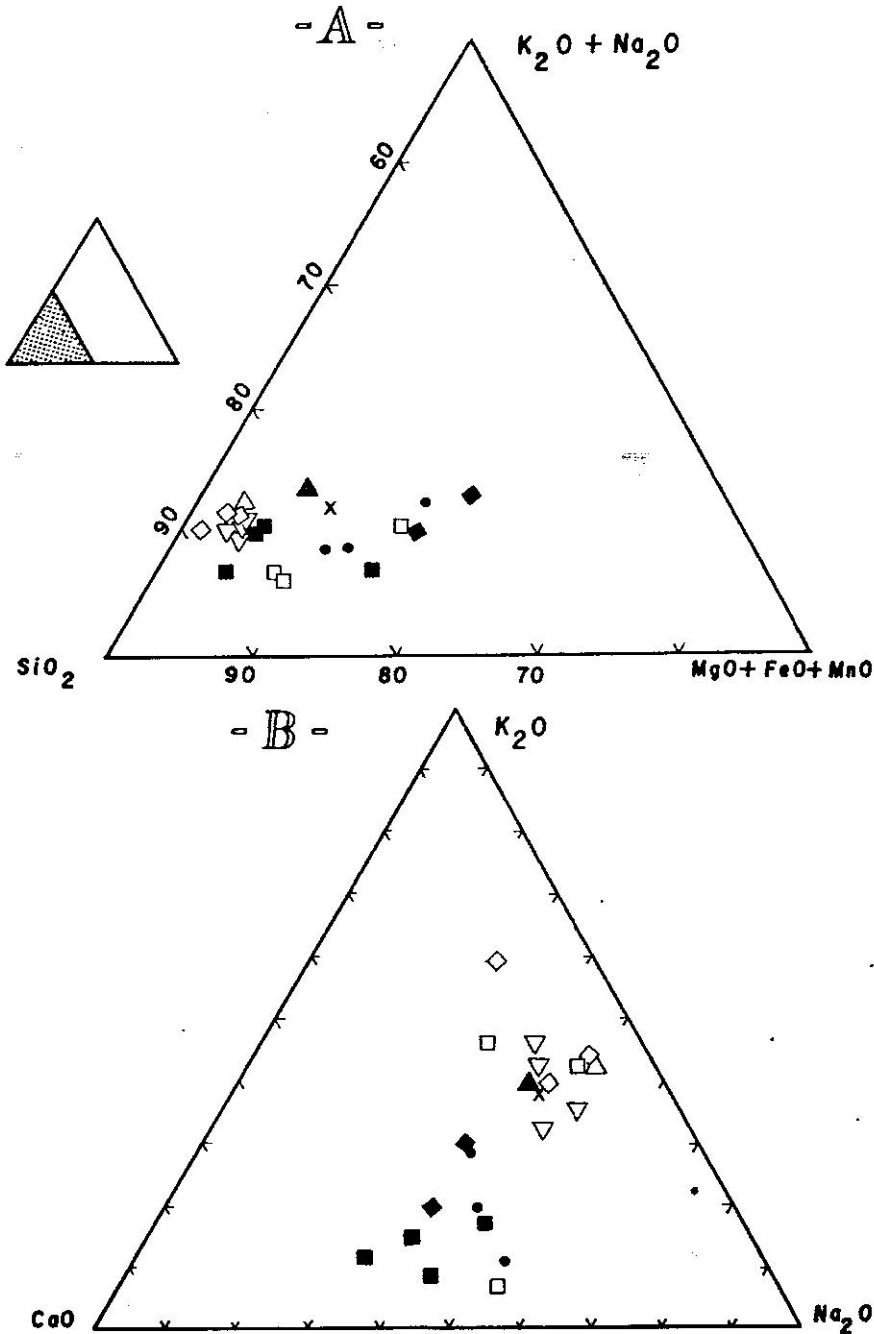


Fig. 7 : $K_2O + Na_2O/SiO_2/MgO + MnO$ diagram (A) and $K_2O/CaO/Na_2O$ diagram (B), for the migmatite leucosomes, paleosomes and biotite gneiss.

Figure 8, Shows the behaviour of Rb, Zr, Sr and Ba with respect to the sum of femic elements to demonstrate their evolution in the different migmatite types. In the low grade migmatites of stromatic type with thin leucosomes and melanosomes, which characterize the initial stage of migmatization, the distribution of Rb and Zr shows a trend corresponding to

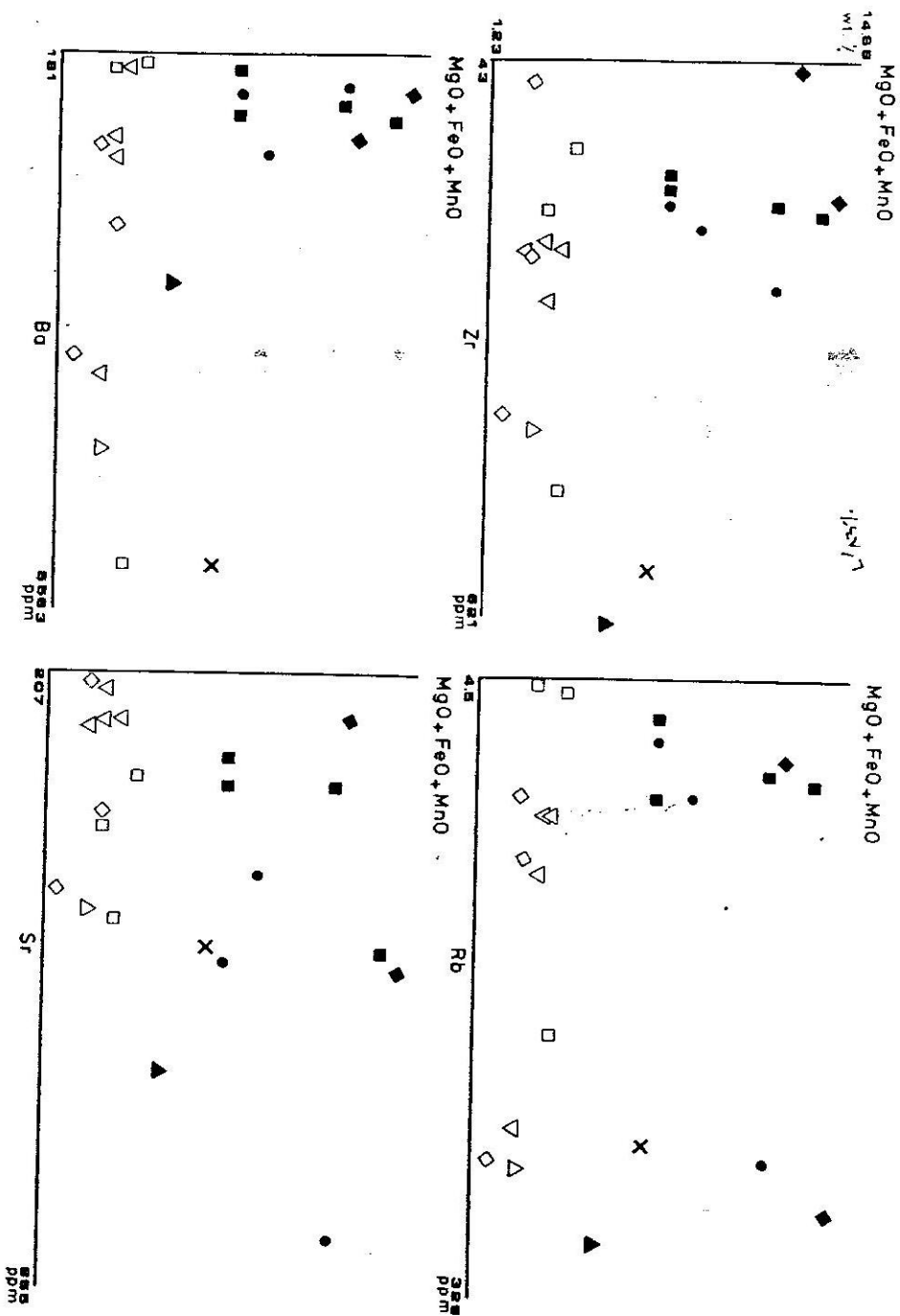


Fig. 8 : Variation diagram of femic oxides ($\text{MgO} + \text{FeO} + \text{MnO}$) versus Zr, Rb, Ba and Sr for the studied migmatites and biotite gneiss.

position. The Behaviour of Ba and Sr. reveals that Sr is more concentrated in paleosome than in leucosome, while Ba is higher in leucosome than in the paleosome. This is different from the general trend discussed by Mehnert and Büsch (op.cit), but still they have mentioned a spread of Ba and Sr in their leucosomes, causing strong deviations. This behaviour of Ba and Sr in the studied migmatites, may be attributed to difference in the original composition of the paleosome, in the degree of migmatization or the possible contamination of the leucosome by the associated melanosome selvages. In the migmatites with banded, boudinage and schlieren types, the leucosomes exhibit a dispersed pattern with respect to Rb, Zr and Ba. These variations are probably related to the later growth of hornblende and biotite or K-Feldspar and plagioclase porphyroblasts.

The plotting of Qz-Or-Ab H_2O system (Fig. 9), shows that the migmatitic leucosomes of boudinage and schlieren types plot rather close to the points of minimum eutectic at moderate water vapour pressures, whereas those of the banded migmatites plot away from the eutectic point at low pressure.

Cluster analysis is carried out for the leucosomes and paleosomes separately, and the linear correlation coefficient is used as similarity criteria showing the affinities between the elements during migmatization and the formation of leucosomes (Table 2a, 2b). The results are portrayed as dendrograms that show a general variation in the geochemical affinities

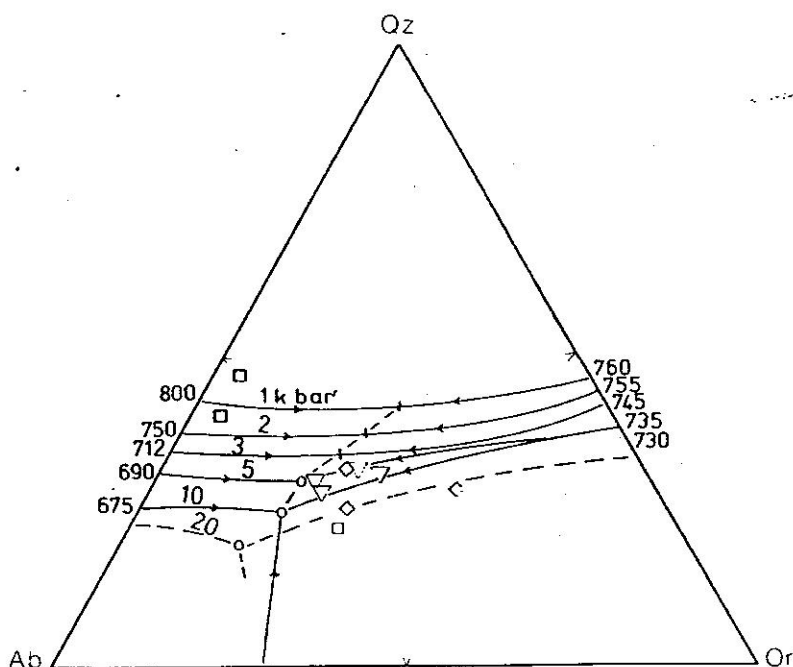


Fig. 9 : Plotting of leucosomes on the H_2O saturated liquidus field boundaries in the system Qz - Ab-Or- H_2O for different water pressures (1,2,3 K bar After Tuttle and Rowen 1958 : 5. 10 K bar After Luth et al.,

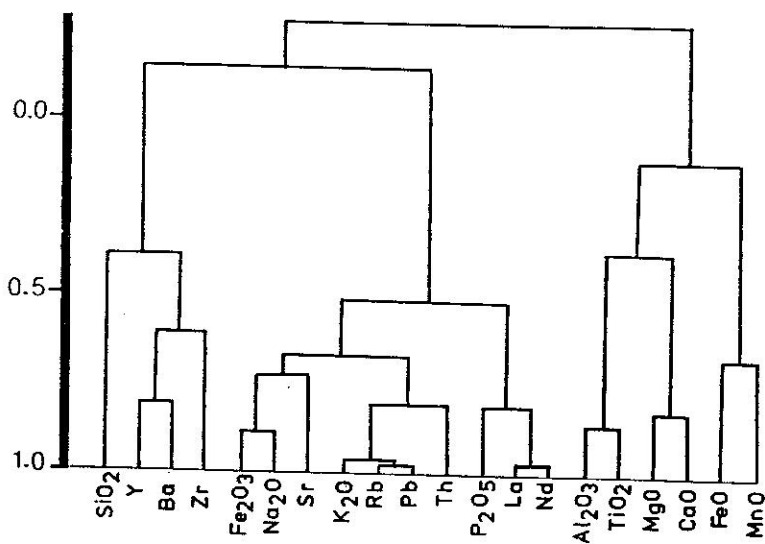
Table 2a

	SiO ₂	Al ₂ O ₃	Fe ₂ O ₃	FeO	MnO	MgO	CaO	Na ₂ O	K ₂ O	TiO ₂	P ₂ O ₅	Rb	Sr	Y	Zr	Ba	La	Nd	Pb	Th
SiO ₂	1.00																			
Al ₂ O ₃	-0.12	1.00																		
Fe ₂ O ₃	-0.34	-0.52	1.00																	
FeO	-0.49	0.26	-0.55	1.00																
MnO	0.58	-0.24	-0.03	0.68	1.00															
MgO	-0.31	0.28	-0.12	0.29	-0.07	1.00														
CaO	-0.46	0.39	-0.24	0.62	0.12	0.82	1.00													
Na ₂ O	-0.41	-0.44	0.89	-0.44	0.01	0.16	-0.05	1.00												
K ₂ O	-0.16	-0.66	0.61	-0.34	0.15	-0.08	-0.40	0.67	1.00											
TiO ₂	0.08	0.86	0.61	0.24	-0.24	0.32	0.46	-0.45	-0.80	1.00										
P ₂ O ₅	0.66	-0.22	0.65	0.04	0.13	0.32	0.40	0.60	0.12	-0.27	1.00									
Rb	-0.10	-0.67	0.73	-0.49	0.01	-0.12	-0.43	0.72	0.96	-0.83	0.19	1.00								
Sr	-0.14	-0.24	0.73	-0.61	0.47	0.09	-0.15	0.75	0.63	0.44	0.42	0.73	1.00							
Y	0.28	-0.45	0.07	-0.27	0.05	-0.11	-0.35	0.08	0.39	0.33	-0.22	0.35	0.06	1.00						
Zr	0.40	-0.27	0.23	-0.61	-0.34	-0.26	-0.59	0.26	0.68	0.39	0.48	0.70	0.51	0.44	1.00					
Ba	0.46	-0.34	-0.04	-0.40	-0.15	-0.18	-0.56	0.06	0.55	0.28	0.54	0.47	0.13	0.81	0.79	1.00				
La	-0.40	-0.53	0.77	-0.24	-0.03	0.00	0.01	0.65	0.52	0.66	0.79	0.60	0.71	0.03	0.03	-0.12	1.00			
Nd	-0.45	-0.36	0.68	-0.14	-0.09	0.05	0.12	0.56	0.35	0.52	0.83	0.49	0.68	0.14	0.11	0.24	0.97	1.00		
Pb	0.01	-0.74	0.69	-0.54	-0.02	-0.20	-0.52	0.69	0.96	0.82	0.11	0.98	0.68	0.45	0.74	0.59	0.56	0.38	1.00	
Th	0.03	-0.78	0.73	-0.56	-0.14	-0.15	-0.42	0.65	0.76	0.80	0.38	0.82	0.66	0.54	0.46	0.47	0.77	0.62	0.86	1.00

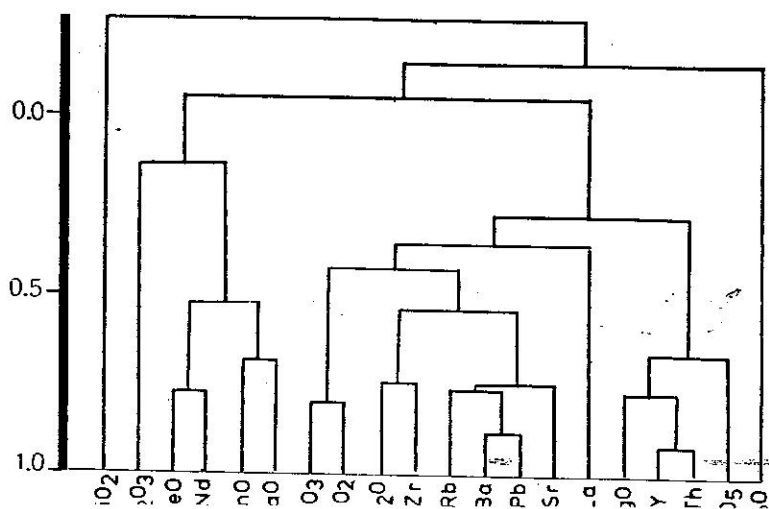
Table 2b

	SiO ₂	Al ₂ O ₃	Fe ₂ O ₃	FeO	MnO	MgO	CaO	Na ₂ O	K ₂ O	TiO ₂	P ₂ O ₅	Rb	Sr	Y	Zr	Ba	La	Nd	Pb	Th
SiO ₂	1.00																			
Al ₂ O ₃	-0.51	1.00																		
Fe ₂ O ₃	-0.70	0.25	1.00																	
FeO	0.16	0.22	-0.43	1.00																
MnO	-0.33	0.12	0.09	0.71	1.00															
MgO	-0.49	-0.27	0.51	-0.11	0.48	1.00														
CaO	0.27	-0.19	-0.05	0.64	0.64	0.20	1.00													
Na ₂ O	-0.18	0.17	0.42	-0.32	-0.16	0.11	0.01	1.00												
K ₂ O	-0.31	0.07	-0.01	-0.52	-0.41	-0.06	-0.88	-0.39	1.00											
TiO ₂	-0.44	-0.18	0.80	-0.36	0.41	0.65	0.11	0.33	-0.16	1.00										
P ₂ O ₅	-0.22	0.01	0.11	0.43	0.54	0.68	0.39	-0.06	-0.33	-0.32	1.00									
Rb	-0.19	-0.13	0.37	-0.91	-0.65	-0.07	-0.73	0.25	0.61	0.29	-0.63	1.00								
Sr	0.03	-0.5	0.44	-0.81	-0.47	0.23	-0.20	0.54	0.03	0.58	-0.33	0.74	1.00							
Y	-0.44	-0.34	0.44	-0.47	-0.07	0.76	-0.27	0.13	0.26	0.67	0.48	0.30	0.45	1.00						
Zr	-0.24	0.03	0.40	-0.74	-0.55	0.17	-0.59	0.73	0.23	0.35	-0.13	0.68	0.69	0.49	1.00					
Ba	-0.31	-0.31	0.45	-0.93	-0.51	0.35	-0.64	0.28	0.57	0.44	-0.26	0.86	0.78	0.66	0.75	1.00				
La	0.04	-0.14	0.26	-0.56	-0.46	0.11	-0.11	0.17	-0.07	0.53	0.25	0.19	0.38	0.55	0.34	0.26	1.00			
Nd	0.01	0.39	0.29	0.77	0.41	0.00	0.29	-0.19	-0.32	-0.29	0.67	-0.82	-0.78	-0.13	-0.36	-0.71	0.30	1.00		
Pb	-0.41	-0.31	0.60	-0.80	-0.37	0.57	-0.46	0.25	0.38	0.69	0.11	0.64	0.71	0.88	0.67	0.87	0.56	0.45	1.00	
Th	-0.39	-0.17	0.48	-0.31	0.00	0.77	-0.09	0.17	0.04	0.67	0.70	0.05	0.30	0.92	0.42	0.44	0.64	0.12	0.77	1.00

between the elements in the paleosomes and leucosomes. In the paleosomes (Fig. 10A), the Al_2O_3 shows an affinity to TiO_2 and MgO to CaO and FeO to MnO , indicating similarity in their geochemical behaviours, as these elements are related to the composition of hornblende and biotite. It can be deduced that the group of elements forming the mafic minerals is the main association as it is related to SiO_2 and the group of trace elements and rare earths. In the leucosomes (Fig. 10B) the affinity of CaO to MnO and Nd to FeO and their relation to Al_2O_3 suggest the formations of hornblende. The TiO_2 shows affinity to Fe_2O_3 reflecting a similar behaviour and their association in biotite and some opaques. K_2O has a rather independent behaviour, due to its mobility, it is mainly related to SiO_2 and Al_2O_3 forming K-feldspars and partly related to biotite. SiO_2 shows no affinity to certain elements, as it is mainly found as free crystallizing quartz or controlling the formation of the different silicates. This is a preliminary attempt to show the general affinity of elements in the fabric units, but still mineral analysis is required to give the exact composition of the different mineral phases during migmatization.



A



B

DISCUSSION AND CONCLUSIONS

In the low grade migmatites, the regular geometry of the leucosomes of stromatic type, the formation of dark melanosomes, the simple metamorphic textures of the paleosome (mesosome), and intermediate position of the chemical composition of the parent rocks between the corresponding leucosomes and paleosomes, suggest that the stromatic migmatite is formed by metamorphic differentiation and segregation in a locally closed system, as described by Yardley (1978); Mehnert and Büsch (1982); McLellan (1983) and Ashworth and McLellan (1985). The coarse grained leucosomes are mainly formed by aqueous fluids escaping during progressive metamorphism (Vidale, 1974 and Yardley 1983) and derived from the surrounding paleosome. This is indicated by the concentration of the stable constituents, as Fe, Mg, Ti and Mn at the margins of the paleosome, forming the melanosome, and extraction and recrystallization of the mobile constituents as Si, Al and Na in the intervening leucosomes. Regarding the distance of migration, Mehnert (1987) suggested that it corresponds to half the vein, on both sides of the leucosome. These leucosomes may be distinguished from the anatectic leucosomes by their pegmatitic habit, as regarded by Yardley (1978). The observed regular harmonic folding is similar to that described by McLellan (1983 and 1984) and indicates metamorphic differentiation and segregation prior to the main deformation.

In discussing the origin of the present banded migmatites, two points are of main interest; the nature and source of the material forming the leucosomes and the reason for localization of these leucosomes in bands and lenses. In the banded gneisses the observed macroscopic and microscopic rhythmic characters reflect primary rock fabrics. The alternating dark and light bands are modified by later growth of hornblende and biotite. This suggests a rhythmic pattern of diffusion of some elements between the bands, mainly in a closed system, which can be explained through the migration of K to the light bands and recrystallization of biotite porphyroblasts, coupled by the migration Ca to the dark bands, reconstitution of hornblende porphyroblasts, and redistribution of Fe and Mg. This process of internal metasomatism through limited migration of elements within few millimeters, suggests mainly solid state diffusion or the occurrence of limited amount of melt. The reconstitution of biotite porphyroblasts, is simply regarded as a process of metamorphic differentiation acting in a closed system. They consume the surrounding older biotite (Bil) during their growth, by small scale diffusion within the quartzofeldspathic bands. This pattern agrees with that of Mehnert (1987) in discussing very short-range chemical migration between alternating bands. In considering the possibility of partial melting, Johannes (1988) discussed that the amount of melt is higher in light neosomes than in mesosomes, as it is controlled by the mineral composition of the bands and the amount of water available. In the light bands with finer grain size, lower amount of Bil and frequent quartz and feldspars, the

leucosome appears to be derived mainly by local partial melting. The form and size of leucosomes depend on the amount of melt produced and the process of melt transfer within the paleosome. In the amphibolitic paleosome, the amount of melt produced is very limited, thus an introduction of water-rich fluids is required to enhance melting and increase the amount of leucosome. The melt produced is transferred either along the foliation planes forming bands or along fault planes and fractures. The migration of leucocratic material along fractures or between breccia fragments, presents an advanced stage of melting and mobilization during migmatization.

The evolution of migmatites of boudinage structure involves ultrametamorphism accompanied by brittle and ductile deformation, through rupturing, flattening and dilatation. The dark bands and boudins are commonly modified by the blastic growth of hornblende or feldspars. They show variation in their chemical composition that reflect variation in their parent rocks and modifications. The associated leucosomes have an eutectic granitic composition and granitic appearance, and suggest partial melting of original quartzofeldspathic material. The granitic melt is the main source of K for the K-feldspar prophyroblasts growing in the associated amphibolites, aided by the K released from the decomposition of biotite during partial melting affecting the boudins.

The described mode of evolution of the ophthalmitic structure suggests a process of local metasomatism, as feldspathization and granitization at different stages of ultrametamorphism. This confirms the general mechanism discussed by King (1950) and Mehnert (1968) for the formation of ophthalmites in mesosomes. McLellan (1983) regarded the ophthalmites as the unsegregated type of migmatites. It can be noticed that the described ophthalmitic structure, partly differs from the ophthalmites of McLellan (op. cit.). Where the present modified paleosomes are found as small lenses surrounded by quartzofeldspathic materials, and appear to result from advanced stages of ductile and brittle deformation, and not as main rock masses.

Migmatites under high-grade conditions, are characterized by granitic or granodioritic leucosomes which require higher PT conditions (Winkler and Breitbart, 1978). The idea that the diatexites represent final stages in the evolution of granitization processes was discussed by Pitcher (1952, 1970); Raugin (1974) and Mehnert (1978). The present schlieren structure may partly result from the progressive delatation and stretching of the dark bands and boudins into roughly parallel streaks floating in quartzofeldspathic material during ultrametamorphism. It may also, represent a primary rock character as heterogeneity in the quartzofeldspathic rocks, containing pelitic or calcipelitic material that develop biotite and hornblende-biotite schists at higher grades. Detailed microscopic examinations of these leucosomes revealed heterogeneity in the textural aspects, having the following genetic implications: (a) grain size: the described leucosomes are mainly fine grained. According to Yardley (1978), the grain size of the leucosome is a good indicator of origin, where the pelitic leucosomes result from partial melting of pelitic

anatexis ; (b) grain shape : it has been observed that the feldspars are mostly equidimensional showing a low aspect ratio . This suggests recrystallization of these leucosomes from partial melts. It also indicates that these leucosome feldspars are not inherited from the paleosomes, which exhibit higher aspect ratio ; (c) grain orientation : the leucosomes show overall gneissose fabric exhibiting preferred orientation of biotite flakes that may be incorporated from the melanosomes, whereas the quartz and feldspars do not develop preferred orientation. This mainly suggests, stress-free crystallization of the leucosomes from melts ; (d) grain distribution : the leucosomes exhibit variation in grain contact relations, they partly show aggregate distribution, with like contacts of similar grains, due to nucleation of new grains at boundaries of the same mineral phase. At a higher degree of partial melting, the leucosomes develop regular-dispersed distribution where unlike contacts between the grains are frequent. They show localized hypidiomorphic granitic texture, having a random distribution, where minerals have no preference for being in contact with each other. This distinguishes melt-grown textures and indicate advanced stages of melting. Although it would be expected from the formed melt in the schlieren type, to have high Rb, Sr and low Ba and Zr, yet the plots of the geochemical data show a different pattern. Here, it should be highly regarded that these leucosomes do not represent a complete homogeneous melt, but rather an high degree of partial melting, where the rocks partly retain their original mineralogical and textural characteristics, and exhibit modifications through segregations and growth of later generations of the mineral phases from the melt. It should be also considered that these leucosomes are highly associated with fine dark melanosomes, which affect their true chemical compositions. Thus these leucosomes should not be looked upon as proper granitic melts undergoing differentiation during crystallization.

From the forementioned discussions, it is seen that the variation in the original composition, physical characters of the parent rocks , degree of melting and deformation control the amount of melt produced and the distribution and form of the generated leucosomes. Considering migmatization through partial melting as an independent process, where geochemical balance is hard to reach, the migmatitic rocks should be treated as governed by their own geochemical rules.

The genetic relation between the present migmatites and the typical Feiran gneiss and migmatite belt, located south of the study area (Schürmann, 1953 ; Akaad, 1959 ; Akaad et al., 1967 a, b; El Gaby, 1967 and El Gaby and Ahmed, 1980), is not yet clear and needs confirmation through further detailed studies.

Acknowledgment

The authors wish to express their thanks for Prof. Dr. M. A. El Sharkawy, Geology Department, Cairo University, for constant encouragement and beneficial

REFERENCES

- AKAAD, M. K. (1959) : The migmatitic gneisses of Wadi Feiran, Sinai Egypt. *Assiut Sci. Techn. Bull.*, 2, 211-237 .
- AKAAD, M. K. , EL-GABY, S. and ABBAS, A. A. (1967 a) : Geology and petrography of the migmatites around Feiran Oasis, Sinai . *Assiut Sci. Techn. Bull.*, 10, 67-87 .
- AKAAD, M. K. , EL-GABY, S. and ABBAS, A. A. (1967b) : On the evolution of Feiran migmatites U.A.R. (Egypt). *J. Geol.*, 11, 49-58.
- ASHWORTH , J. R. (1979) : Comparative petrography of deformed and undeformed migmatites from the Grampian Highlands, Scotland. *Geol. Mag.*, 116, 6, 445-456 .
- ASHWORTH and MCLELLAN, E. L. (1985) : Textures. In : *Migmatites* (Ashworth, J. R. ed.) Blackie and Son Ltd., 180- 203 .
- BUSCH, W. SCHNEIDER, G. and MEHNERD, K.R. (1974) : Initial melting at grain boundaries, part II : Melting in rocks of granodioritic, quartzdioritic and tonalitic composition. *Neues Jb. Mineral. Mh.*, 345-370 .
- EL-GABY, S. (1976) : The mode of formation of cordierite gneisses in migmatitic rocks. *Assiut Sci. Techn. Bull.*, 10, 91 - 106 .
- EL-GABY, S. and AHMED, A. A. (1980) : The Feiran - Solaf gneiss belt, SW of Sinia, Egypt. In : *Evolution and Mineralization of the Arabian - Nubian Shield*. *Inst. App. Geol. (Jeddah), Bull.*, 3, 95 - 105 .
- GUPTA, L. N. and JOHANNES, W. (1982) : Petrogenesis of a stromatic migmatite (Nelaug, southern Norway) . *J. Petrol.*, 23, 548-567
- HENKES, L. and JOHANNES, W. (1981) : The petrology of a migmatite (Arvika, Varmland, western Sweden). *Neues Jb. Miner. Abh.*, 141, 413 - 133 .
- HOLMQUIST, P.J. (1907) : Adergneisbildung und magmatische Assimilation in Grundgebirge Schwedens. *Geol. Foren. Stockholm Forth.*, 29, 313 - 354 .
- HOLMQUIST, P.J. (1921) : Typen und Nomenklatur der Asergesteine. *Geol. Foren. Stockh Forh.*, 43, 612-631 .
- JOHANNES , W. (1988) : What controls partial melting in migmatites ? . *J. metamorphic Geol.*, 6, 451 - 465 .
- JOHANNES, W. and GUPTA, L.N. (1982) : Origin and evolution of a migmatite. *Contrib Miner. Petrol.*, 79, 114 - 123 .
- JOHANNES, W. and GUPTA, L.N. (1983) : On the origin of stromatic (layered) migmatites. In : *Migmatites, Melting and Metamorphism*, (Atherton, M.P. and Gribble, C.D., eds.) Shiva, Nantwich, 234 - 248 .
- JOHANNES, W. and GUPTA, L.N., (1986) : Migmatites : Examples from Arvika and Graestorp (western Sweden) and Nelaug (southern Norway) areas, results of almost isochemical partial melting. *Sci. Geol., Bull.*, 39, 4, 381-390, Strasbourg .
- KING, B.C. (1950) : Some large feldspar augen from near Ilorin Town, Nigeria. *Geol. Mag.*, 87, 369 - 372 .
- LUTH, W.C.; JANNIS, R.H. and TUTTLE, O. F. (1964) : The granite system at pressure of 4 to 10 Kilobars. *J. Geophys. Res.* 69 759 - 773

- MCLELLAN, E.L. (1983) : Contrasting textures in metamorphic and anatectic migmatites; an example from the Scottish Caledonides. *J. Metamorphic Geol.*, 1, 241 - 262 .
- MCLELLAN, E.L. (1984) : Deformational behaviour of migmatites and Problems of structural analysis in migmatite terrains. *Geol. Mag.*, 121 , 339 - 345 .
- MEHNERT, K.R. (1953) : Petrographie und Abfolge der Granitisation in Schwarzwald . *Neus Jb. Mineral.*, 85 , 59 - 140 .
- MEHNERT, K.R. (1963) : Petrographie und Abfolge der Granitisation in Schwarzwald *Neus Jb. Mineral.*, 99, 161- 199 .
- MEHNERT, K.R. (1968) : Migmatites and the origin of Granitic Rocks. Elsevier , Amsterdam, 405 P.
- MEHNERT, K.R. (1987) : The granitization problem-revisited: *Fortschr. Miner.*, 65, 2, 285-306 . , Stuttgart .
- MEHNERT, K.R. and BUSCH W. (1982) : The initial stage of migmatite formation. *Neues. Jb. Mineral., Abh.*, 145, 211 -238 .
- MICHEL-LEVY, A. (1893) : Contribution à l'étude du granite de Flamenville et des granites français en general . *Bull. Serv. Carte Geol.*, France, 5, 36 : 317 .
- PITCHER, W.S. (1952) : The migmatitic older granodiorite of Thorp district, Co. Donegal. *Quart. J. Geol. Soc.*, London 108, 413 - 446 .
- PITCHER, W.S. (1970) : Ghost stratigraphy in intrusive granites : a review. - *Geol. J.*, Liverpool, Spec. Issue, 2, 123 - 140 .
- RAUGIN, E. (1974) : Les caractères des granites autochtones. *Krystallinikum*, 10, 7-18 .
- SCHURMANN, H. M. E. (1953) : The Precambrian of the Gulf of Suez Area. *Comptes Rendus Inter. Geol. Cong.*, Alger., Sect. I, Fasc. I, 115-135 .
- SEDERHOLM, J. J. (1907) : Om granit och gneis. *Bull. Comm. Geol.*, Finl., 23 P.
- SEDERHOLM, J. J. (1934) : On migmatites and associated Precambrian rocks of south western Finland. *Bull. Comm. Geol.*, Finland, 107, 1-68.
- TUTTLE, O.F. and BOWEN, N. L. (1985) : Origin of granite in the light of experimental studies in the system $\text{Na Al Si}_3\text{O}_8$ - $\text{K Al Si}_3\text{O}_8$ - SiO_2 - H_2O . *Geol. Soc. Am. Mem.*, 74, 153.
- VIDALE, R. J. (1974) : Vein assemblages and metamorphism in Dutchess County, New York. *Geol. Soc. Am. Bull.*, 85, 303 - 306 .
- WINKLER, H.G.F. (1961) : On coexisting feldspars and their temperature of crystallization. *Cursillos Conf. Inst. "Lucas Mallada"*, 8, 9-13 .
- WINKLER, H.G.F. (1979) : Petrogenesis of Metamorphic rocks . Springer-Verlag, New York, London 348 P.
- WINKLER, H.G.F. and BREITBART, R. (1978) : New aspects of granitic magmas. *Neues Jb. Mineral. Abh.*, 463-480 .
- YARDLEY, B.W.D. (1978) : Genesis of the Skagit Gneiss migmatites, Washington, and the distinction between possible mechanisms of migmatization. *Geol. Soc. Am. Bull.*, 89, 941-951 .
- YARDLEY, B.W.D. (1983) : Quartz veins and devolatilization during